Using marginal impedance distributions to calibrate impedance functions for accessibility measurement: a theoretical and empirical analysis

Harry Roberts*[1], Chiara Calastri[2], and Richard Batley[3]

[1]PhD Candidate, Institute for Transport Studies, University of Leeds, UK
[2]Associate Professor, Institute for Transport Studies, University of Leeds, UK
[3]Professor of Transport Demand and Valuation, Institute for Transport Studies, University of Leeds, UK

Short summary

An essential component of any accessibility measure is an impedance function capturing the frictional impact of travel on activity participation. Such functions are commonly calibrated using the marginal distribution of the impedance variable, usually distance or time. However, this approach lacks a clear theoretical basis, and is affected by bias related to the fact that shorter trips have fewer available destinations than longer trips, meaning that trips with low impedance occur less frequently. This bias may explain the observed bell-shaped survival functions for impedance, which are often attributed to frictionless responses at lower impedance values. This paper develops a theoretical foundation for calibration to marginal impedance distributions, proposing a power function correction to isolate the bias from the impedance function during estimation. Empirical results show that applying near-linear correction terms leads to better-fitting distributions. The resultant impedance functions exhibit steeper decay, carrying important implications for accessibility measurement and policy interpretation.
Keywords: Accessibility measurement, Calibration techniques, Impedance functions, Land-use planning, Transport equity, Transport network modelling.

1 Introduction

Accessibility measures quantify a location's potential for interaction with other locations in space, considering both the opportunities they contain and the effort required to travel between them (Hansen, 1959; Miller, 2020). These measures typically incorporate both the magnitude of opportunity at each available location and the *impedance*, or generalised cost, of travelling there using the transport network, commonly represented by distance or travel time. A standard formulation expresses accessibility as the weighted sum

$$A_i = \sum_{j \in D_i} y_j f(x_{ij}) \tag{1}$$

where A_i denotes the accessibility of location i, D_i is the set of reachable locations, y_j is the magnitude of opportunity at j, x_{ij} is the impedance between i and j, and $f(x_{ij})$ is the *impedance function*, capturing how impedance affects trip-making propensity independently of destination characteristics.

Various functional forms have been proposed for $f(\cdot)$, with two common examples being the negative exponential $f(x) = e^{-\lambda x}$ and Gaussian $f(x) = e^{-(\lambda x)^2}$ (Ingram, 1971; Dalvi & Martin, 1976). The choice of functional form implicitly reflects assumptions about travel behaviour; for example, the Gaussian's initial concavity implies a relatively frictionless response at low impedance (Vale & Pereira, 2017). In all cases, parameters such as λ must either be specified heuristically (Guy, 1983; Vale & Pereira, 2017) or estimated empirically.

Two broad approaches are used to estimate impedance function parameters. In *Trip Matrix Calibration* (TMC) a trip distribution model incorporating the chosen impedance function is calibrated to an observed origin–destination matrix (Parks, 2004; Scott & Horner, 2008; Caschili et al., 2015; Piovani et al., 2018). This approach is grounded in the entropy-maximisation framework of Wilson (1967, 1971) and reconciles directly with the spatial distribution of observed trips. By contrast,

Impedance Distribution Calibration (IDC) estimates the impedance function from the marginal distribution of impedance values across all trips (Kwan, 1998; Shen, 1998; Wu et al., 2019; Department for Transport, 2025). IDC is simpler to implement, requiring only aggregated distributional data, and is therefore widely used in practice despite lacking a formal theoretical foundation.

The appeal of IDC lies in the intuition that the influence of impedance on trip-making should be reflected in the marginal distribution of impedance over observed trips. However, this distribution also depends on the spatial configuration of destinations, which may introduce structural bias (Iacono et al., 2008). Observed impedance distributions often exhibit increasing density at low values of impedance, as illustrated in Figure 1, which is inconsistent with a monotonically decreasing impedance function (Verma & Ukkusuri, 2025). To address this, several studies calibrate impedance functions to the survival function, which is necessarily decreasing by construction (Ingram, 1971; Vale & Pereira, 2017; Verma & Ukkusuri, 2025). Ingram (1971) interprets the resulting bell-shaped survival curve as support for using a Gaussian impedance function.

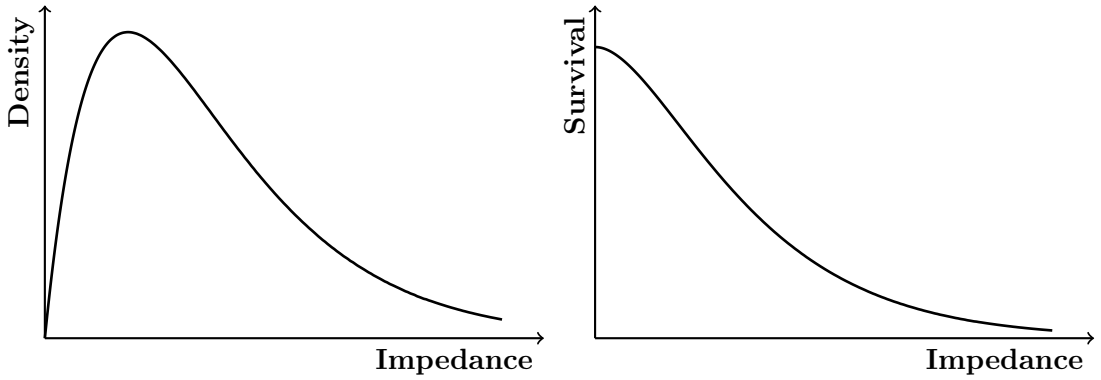


Figure 1: Illustrative sketches of a typical density function (left) and survival function (right) for a marginal impedance distribution.

Given the widespread use of IDC to select impedance functional forms, and that the choice of form implies a hypothesis of travel behaviour, a clearer understanding of the underlying mechanics of this approach is required. This study therefore addresses three research questions:

1. Does a theoretical basis exist for calibrating impedance functions to marginal impedance distributions?
2. Does spatial structure introduce bias into marginal impedance distributions, and how can this bias be corrected for?
3. Why do marginal impedance distributions often exhibit increasing density at low values?

This is achieved through a theoretical analysis, supported by empirical validation.

2 Theory

Following Wilson (1967, 1971), the distribution of trips T_{ij} from origins i to destinations j is described by the doubly-constrained gravity model

$$T_{ij} = A_i O_i B_j D_j f(x_{ij}), \quad A_i = \frac{1}{\sum_j B_j D_j f(x_{ij})}, \quad B_j = \frac{1}{\sum_i A_i O_i f(x_{ij})} \tag{2}$$

where $f(x_{ij})$ is the impedance function, O_i and D_j denote the total number of trips originating at i and ending at j respectively, and A_i and B_j are balancing factors. This formulation underpins estimation in the TMC approach identified in Section 1.

The marginal distribution of impedance values can be written as

$$\varphi(x) = \sum_{ij} T_{ij} \delta_{x_{ij} x} = \sum_{ij} A_i O_i B_j D_j f(x_{ij}) \delta_{x_{ij} x} \tag{3}$$

where $\delta_{x_{ij}x} = 1$ if $x_{ij} = x$ and $\delta_{x_{ij}x} = 0$ otherwise. Since the summand is non-zero only for pairs with $x_{ij} = x$, this expression can be factorised as

$$\varphi(x) = \omega(x) f(x), \qquad \omega(x) = \sum_{ij} A_i O_i B_j D_j \delta_{x_{ij}x} \tag{4}$$

where $\omega(x)$ aggregates the origin- and destination-specific weights across all pairs with impedance x. The term $\omega(x)$ therefore captures structural bias arising from the spatial configuration of opportunities.

Defining $\mu(x)$ to be the mean of $A_i O_i B_j D_j$ conditional on $x_{ij} = x$, $\omega(x)$ can be restated as

$$\omega(x) = N(x)\mu(x) \tag{5}$$

with $N(x)$ being the number of i–j pairs with impedance x. The origin and destination weights A_i, O_i, B_j, D_j are specified as location-specific and are accordingly assumed to be independent of the pairwise impedance x_{ij} in aggregate. Under this assumption, $\mu(x)$ does not vary systematically with x, implying that $\omega(x)$ can be modelled as proportional to $N(x)$.

If origins and destinations are uniformly distributed in a two-dimensional impedance space, $N(x)$ grows linearly with x, being proportional to the circumference of the locus of radius x around each origin. Figure 2 illustrates this geometrically for 1,000 uniformly distributed destinations over a $10\,\text{km}^2$ area, with Euclidean distance treated as impedance. The number of available destinations approximately doubles when the impedance radius doubles, demonstrating linear growth.

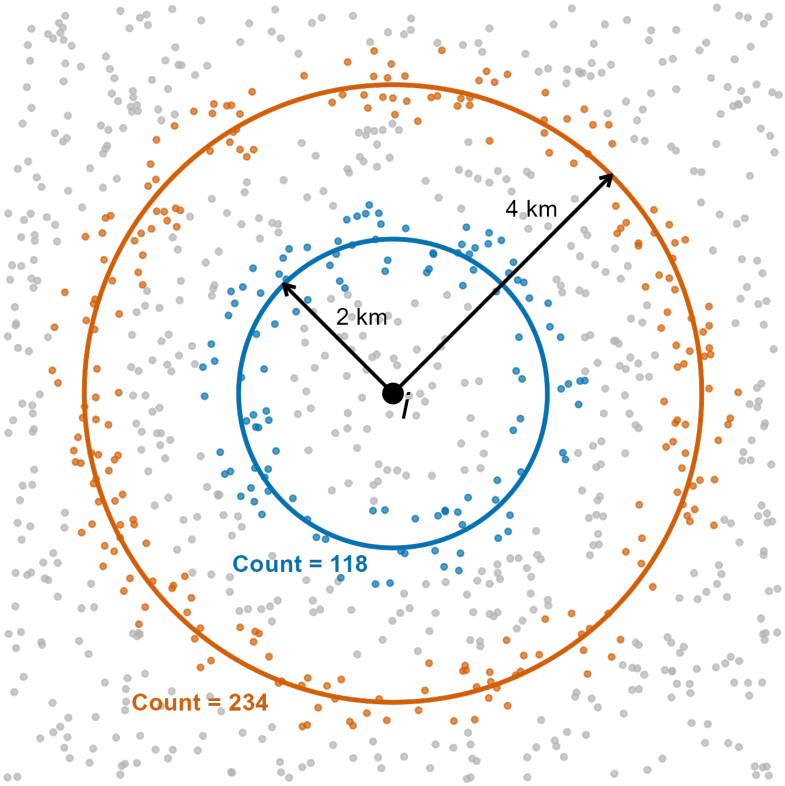


Figure 2: Illustration of linear growth in destinations with Euclidean distance, with 1000 uniformly distributed destinations over a $10\,\text{km}^2$ area.

More generally, if destinations are not uniformly distributed and instead occupy an effective spatial dimension of $1 \leq \beta \leq 2$ determined by the extent of spatial clustering (see Falconer (2013) for further detail on non-integral dimensional geometry), the number of origin–destination pairs with impedance x scales as $x^{\beta-1}$. Applying the correction $\omega(x) \propto x^{\beta-1}$ yields the distribution

$$\varphi(x) \propto x^{\beta-1} f(x) \tag{6}$$

where β is a parameter to be estimated. Not applying this correction corresponds to the implicit assumption $\beta = 1$, under which the density of available destinations does not increase with impedance, as would occur if all locations were distributed along a single, one-dimensional road.

In intuitive terms, longer trips generally offer access to a larger set of destinations, and this structural effect must be separated from behavioural distance decay during estimation. This explains the initially increasing density in observed marginal impedance distributions, prior to the point at which decay becomes dominant. Consequently, a bell-shaped survival function does not uniquely imply a Gaussian impedance function, as previously suggested by Ingram (1971), but may instead arise from the scarcity of destinations at low levels of impedance.

3 Methodology

A dataset of observed trip travel times is used to empirically evaluate the calibration framework introduced in Section 2. The data is drawn from the 2002–2019 UK National Travel Surveys (Department for Transport, 2026), over which a total of 304,945 participants recorded travel times and purpose for 4,866,698 trips undertaken within seven-day diary periods. For the present analysis, the dataset is restricted to 405,062 home-to-work trips only, as accessibility measures are generally purpose-specific (Miller, 2020), thus the origins are homes and the destinations are workplaces.

Impedance is modelled using a flexible power exponential function

$$f(t) = e^{-(\lambda t)^r} \tag{7}$$

where $t > 0$ denotes travel time, $\lambda > 0$ is a scale parameter, and $r > 0$ governs the functional form of decay. Incorporating the spatial bias correction term and normalising yields the generalised gamma distribution

$$\varphi(t) = \frac{r\lambda^\beta}{\Gamma(\beta/r)} t^{\beta-1} e^{-(\lambda t)^r} \tag{8}$$

where the parameter $1 \leq \beta \leq 2$ captures the effective spatial dimension of homes and workplaces. The corresponding survival function is

$$S(t) = \frac{\Gamma(\beta/r, (\lambda t)^r)}{\Gamma(\beta/r)} \tag{9}$$

with $\Gamma(\cdot, \cdot)$ denoting the upper incomplete gamma function.

Three specifications are considered for the impedance exponent r: $r = 1$, corresponding to a negative exponential form; $r = 2$, corresponding to a Gaussian form; and r estimated freely. Likewise, three specifications are examined for the spatial bias parameter β: $\beta = 1$, representing no bias correction; $\beta = 2$, implying linear growth in impedance space; and β estimated freely. Interacting these assumptions yields nine candidate models, summarised in Table 1.

Each model is estimated using maximum likelihood, implemented via the `maxLik` package in R (Henningsen & Toomet, 2011). Analytical gradients and Hessians allow optimisation via the Newton—Raphson algorithm. When r is fixed, the log-likelihood is globally concave over $t > 0$, ensuring a unique maximum for Models A–F. In contrast, Models G–I, for which r is estimated freely, may exhibit local maxima. To address this, estimation for these models is repeated from multiple starting values (1, 1.5, and 2) for both r and β.

Models are fitted using a random 80% subsample of observed trips and evaluated on a 20% validation sample. Model fit is assessed using the in-sample log-likelihood $\ln \hat{l}$, which is reported alongside the corresponding Akaike Information Criterion, $\text{AIC} = 2k - 2\ln \hat{l}$, where k is the number of estimated parameters. Predictive performance is evaluated using the log-likelihood on the validation sample. In addition, to facilitate comparison with earlier empirical studies (Vale & Pereira, 2017; Verma & Ukkusuri, 2025), each model's predicted survival function is compared with the empirical survival curve from the validation sample, and a corresponding R^2 is computed as a descriptive measure of curve agreement.

Table 1: Candidate distributions.

Model	r	β	$f(t)$	$\omega(t) \propto$	$\varphi(t)$	$S(t)$
A	1	1	$e^{-\lambda t}$	1	$\lambda e^{-\lambda t}$	$e^{-\lambda t}$
B	1	2	$e^{-\lambda t}$	t	$\lambda^2 t e^{-\lambda t}$	$(1+\lambda t)e^{-\lambda t}$
C	1	Free	$e^{-\lambda t}$	$t^{\beta-1}$	$\frac{\lambda^\beta}{\Gamma(\beta)} t^{\beta-1} e^{-\lambda t}$	$\frac{\Gamma(\beta,\lambda t)}{\Gamma(\beta)}$
D	2	1	$e^{-(\lambda t)^2}$	1	$\frac{2\lambda}{\sqrt{\pi}} e^{-(\lambda t)^2}$	$\mathrm{erfc}(\lambda t)$
E	2	2	$e^{-(\lambda t)^2}$	t	$2\lambda^2 t e^{-(\lambda t)^2}$	$e^{-(\lambda t)^2}$
F	2	Free	$e^{-(\lambda t)^2}$	$t^{\beta-1}$	$\frac{2\lambda^{\beta/2}}{\Gamma(\beta/2)} t^{\beta-1} e^{-(\lambda t)^2}$	$\frac{\Gamma(\beta/2,(\lambda t)^2)}{\Gamma(\beta/2)}$
G	Free	1	$e^{-(\lambda t)^r}$	1	$\frac{r\lambda}{\Gamma(1/r)} e^{-(\lambda t)^r}$	$\frac{\Gamma(1/r,(\lambda t)^r)}{\Gamma(1/r)}$
H	Free	2	$e^{-(\lambda t)^r}$	t	$\frac{r\lambda^2}{\Gamma(2/r)} t e^{-(\lambda t)^r}$	$\frac{\Gamma(2/r,(\lambda t)^r)}{\Gamma(2/r)}$
I	Free	Free	$e^{-(\lambda t)^r}$	$t^{\beta-1}$	$\frac{r\lambda^\beta}{\Gamma(\beta/r)} t^{\beta-1} e^{-(\lambda t)^r}$	$\frac{\Gamma(\beta/r,(\lambda t)^r)}{\Gamma(\beta/r)}$

4 Results and discussion

Estimated parameters and in-sample fit statistics are reported in Table 2, with out-of-sample validation results shown in Table 3. All models converged with parameter estimates in their expected domains except for model I, which is excluded from further analysis. Model fit and predictive performance rankings are consistent, with in-sample and validation log-likelihoods yielding identical orderings, and the survival R^2 only differing in its placement of Model D.

Table 2: Model parameter estimates and in-sample statistics.

Model	k	$\hat{r}$ (s.e.)	$\hat{\beta}$ (s.e.)	$\hat{\lambda}$ (s.e.)	$\ln \hat{l}$	AIC
A	1	1	1	0.0354 (0.0000)	-1,406,378	2,812,759
B	1	1	2	0.0709 (0.0000)	-1,370,321	2,740,644
C	2	1	1.968 (0.005)	0.0698 (0.0001)	-1,370,297	2,740,598
D	1	2	1	0.0196 (0.0000)	-1,397,429	2,794,860
E	1	2	2	0.0277 (0.0000)	-1,430,701	2,861,404
F	2	2	1.146 (0.002)	0.0212 (0.0000)	-1,394,211	2,788,425
G	2	1.585 (0.004)	1	0.0229 (0.0000)	-1,393,556	2,787,116
H	2	0.881 (0.002)	2	0.0927 (0.0006)	-1,369,100	2,738,205

Table 3: Validation statistics.

Model	$\ln \hat{l}$	Survival R^2
A	-351,734	0.976292
B	-342,806	0.996506
C	-342,797	0.996581
D	-349,541	0.989445
E	-357,990	0.956743
F	-348,761	0.988160
G	-348,555	0.989364
H	-342,487	0.996930

A key result is the substantial impact of spatial bias correction on the estimated decay rate. Introducing a linear or free bias correction causes $\hat{\lambda}$ to increase markedly, nearly doubling relative

to uncorrected specifications in the negative exponential case. This implies a much steeper decay in destination weighting, suggesting that bias correction may materially affect accessibility measurement outcomes.

The preferred strength of bias correction depends on the assumed impedance form. Under a negative exponential impedance, models incorporating strong bias correction perform best. Models B and C clearly outperform the uncorrected Model A, with Model C estimating $\hat{\beta} = 1.968$, close to the linear benchmark. For Gaussian impedance functions, weaker correction is favoured: Model D outperforms Model E, and Model F estimates $\hat{\beta} = 1.146$, closer to unity. This likely reflects the Gaussian's bell-shaped form, which more closely matches the empirical density near its peak and therefore attracts less correction.

Among models with free r, Model G estimates $\hat{r} = 1.585$ without bias correction, between the exponential and Gaussian cases. Model H, however, achieves the strongest fit by combining linear bias correction with $\hat{r} = 0.881$, indicating sub-exponential decay.

Figure 3 compares modelled survival functions with the observed survival curve. Models B, C, and H most closely reproduce both the initial curvature and subsequent decay observed in the data. Across specifications, survival probabilities in the tail tend to be underestimated, which may indicate unmodelled heterogeneity in individuals' impedance sensitivities.

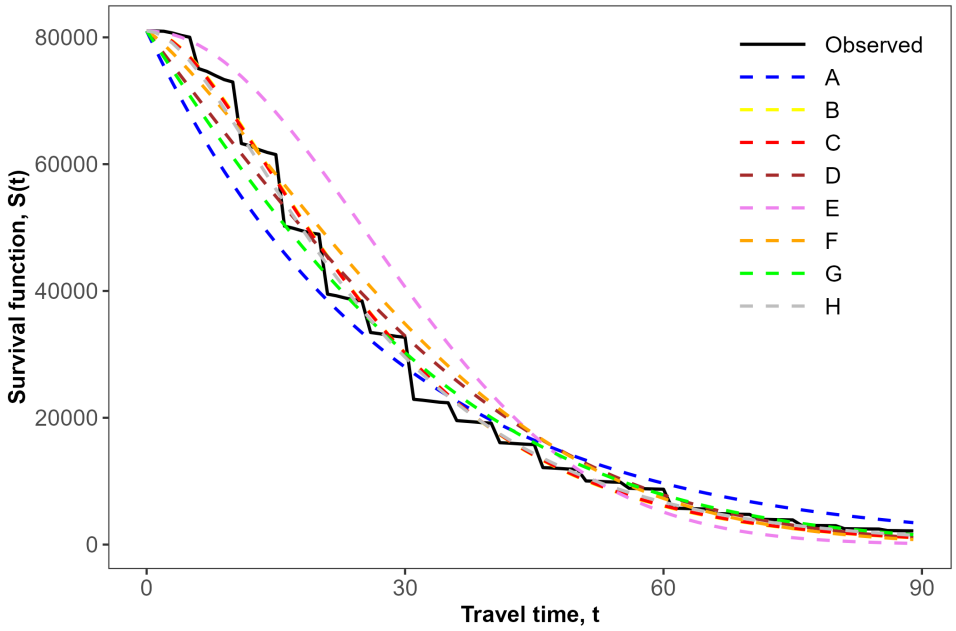


Figure 3: Survival functions for each model plotted against the observed survival curve

Figure 4 presents the corresponding impedance functions after removing the bias term $\omega(t)$ and normalising to $f(0) = 1$. The strongest models (B, C, and H) all exhibit considerably steeper decay than uncorrected alternatives, reinforcing the conclusion that spatial bias correction has substantial behavioural and practical implications for accessibility measures.

Overall, models with $r \approx 1$ and $\beta \approx 2$ provide the best representation of observed trip behaviour. This supports the use of a near-linear bias correction and a negative exponential or slightly sub-exponential impedance function. In the absence of bias correction, Gaussian impedance forms perform better, consistent with earlier empirical studies.

5 Conclusions

This study developed a theoretical foundation for Impedance Distribution Calibration as a method for estimating impedance function parameters, and demonstrated the need to account explicitly for a spatial bias term arising from the distribution of opportunities that is distinct from the impedance function itself. It was hypothesised the bell-shaped survival functions commonly ob-

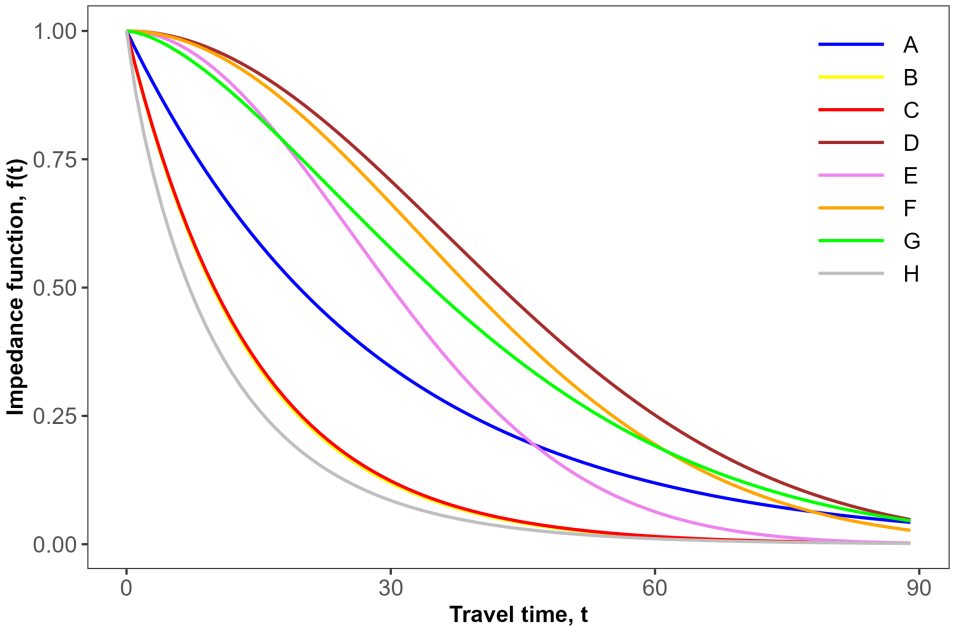


Figure 4: Corresponding impedance functions for each model

served in marginal impedance distributions may be attributed to this structural effect, rather than implying a frictionless behavioural response at low impedance values.

The empirical results show that applying a linear or near-linear spatial bias correction in combination with a negative exponential or sub-exponential impedance function produces distribution models with superior fit and predictive performance than both uncorrected and Gaussian-type specifications. Importantly, the introduction of the bias correction substantially alters the estimated impedance functions, producing markedly steeper decay profiles.

These findings suggest that commonly used impedance functions may understate the rate at which interaction potential declines with increasing travel impedance if spatial bias is ignored. The implications for accessibility measurement are therefore non-trivial: measures with steeper decay in the impedance function apply greater weight to closer locations, meaning that zones with opportunities that are very nearby are assigned a higher accessibility relative to those with a larger number of more distant opportunities. Such measures may lend support to land-use-oriented planning approaches that prioritise proximity, such as fifteen-minute city concepts.

A key limitation of this study is the lack of consideration of both individual-level heterogeneity and the impact of mode choice, although there is an intention to expand the scope of this work to include those topics.

Acknowledgements

This work was supported by UKRI and Network Rail through the ESRC White Rose DTP collaborative studentship programme.

References

Caschili, S., De Montis, A., & Trogu, D. (2015). Accessibility and rurality indicators for regional development. *Computers, Environment and Urban Systems*, *49*, 98–114. doi: 10.1016/j.compenvurbsys.2014.05.005

Dalvi, M. Q., & Martin, K. M. (1976). The measurement of accessibility: Some preliminary results. *Transportation*, *5*(1), 17–42. doi: 10.1007/BF00165245

Department for Transport. (2025). *Transport connectivity metric* (Tech. Rep.). UK Government. Retrieved 2026-04-02, from `https://www.gov.uk/government/publications/transport-connectivity-metric/transport-connectivity-metric`

Department for Transport. (2026). *National Travel Survey, 2002-2024.* UK Data Service. doi: 10.5255/UKDA-SN-5340-15

Falconer, K. (2013). *Fractal Geometry* (3rd ed.). Chichester: Wiley.

Guy, C. M. (1983). The Assessment of Access to Local Shopping Opportunities: A Comparison of Accessibility Measures. *Environment and Planning B: Planning and Design*, *10*(2), 219–237. doi: 10.1068/b100219

Hansen, W. G. (1959). How Accessibility Shapes Land Use. *Journal of the American Institute of Planners*, *25*(2), 73–76. doi: 10.1080/01944365908978307

Henningsen, A., & Toomet, O. (2011). maxLik: A package for maximum likelihood estimation in R. *Computational Statistics*, *26*(3), 443–458. doi: 10.1007/s00180-010-0217-1

Iacono, M. J., Krizek, K. J., & El-Geneidy, A. M. (2008). *Access to Destinations: How Close Is Close Enough? Estimating Accurate Distance Decay Functions for Multiple Modes and Different Purposes*. St. Paul, MN: Minnesota Department of Transportation. Retrieved 2026-04-13, from `https://mdl.mndot.gov/items/200811` (Number: MN/RC 2008-11)

Ingram, D. (1971). The Concept of Accessibility: A Search for an Operational Form. *Regional Studies*, *5*, 101–107. doi: 10.1080/09595237100185131

Kwan, M.-P. (1998). Space-Time and Integral Measures of Individual Accessibility: A Comparative Analysis Using a Point-based Framework. *Geographical Analysis*, *30*(3), 191–216. doi: 10.1111/j.1538-4632.1998.tb00396.x

Miller, E. J. (2020). *Measuring Accessibility: Methods and Issues* (Vol. 2020/25). Paris: OECD Publishing. doi: 10.1787/8687d1db-en

Parks, V. (2004). Access to Work: The Effects of Spatial and Social Accessibility on Unemployment for Native-Born Black and Immigrant Women in Los Angeles. *Economic Geography*, *80*(2), 141–172. doi: 10.1111/j.1944-8287.2004.tb00305.x

Piovani, D., Arcaute, E., Uchoa, G., Wilson, A., & Batty, M. (2018). Measuring accessibility using gravity and radiation models. *Royal Society Open Science*, *5*(9), 171668. doi: 10.1098/rsos.171668

Scott, D., & Horner, M. (2008). Examining the role of urban form In shaping people's accessibility to opportunities: An exploratory spatial data analysis. *Journal of Transport and Land Use*, *1*(2). doi: 10.5198/jtlu.v1i2.25

Shen, Q. (1998). Location Characteristics of Inner-City Neighborhoods and Employment Accessibility of Low-Wage Workers. *Environment and Planning B: Planning and Design*, *25*(3), 345–365. doi: 10.1068/b250345

Vale, D. S., & Pereira, M. (2017). The influence of the impedance function on gravity-based pedestrian accessibility measures: A comparative analysis. *Environment and Planning B: Urban Analytics and City Science*, *44*(4), 740–763. doi: 10.1177/0265813516641685

Verma, R., & Ukkusuri, S. V. (2025). What determines travel time and distance decay in spatial interaction and accessibility? *Journal of Transport Geography*, *122*, 104061. doi: 10.1016/j.jtrangeo.2024.104061

Wilson, A. G. (1967). A statistical theory of spatial distribution models. *Transportation Research*, *1*(3), 253–269. doi: 10.1016/0041-1647(67)90035-4

Wilson, A. G. (1971). A Family of Spatial Interaction Models, and Associated Developments. *Environment and Planning A: Economy and Space*, *3*(1), 1–32. doi: 10.1068/a030001

Wu, X., Lu, Y., Lin, Y., & Yang, Y. (2019). Measuring the Destination Accessibility of Cycling Transfer Trips in Metro Station Areas: A Big Data Approach. *International Journal of Environmental Research and Public Health*, *16*(15), 2641. doi: 10.3390/ijerph16152641